Lattice dynamics of silicon oxynitride, Si_2N_2O: vibrational spectrum, elastic and piezoelectric properties

1989 J. Phys.: Condens. Matter 1 10053

(http://iopscience.iop.org/0953-8984/1/50/008)

J. Phys.: Condens. Matter **1** (1989) 10053–10066. Printed in the UK

Lattice dynamics of silicon oxynitride, Si_2N_2O: vibrational spectrum, elastic and piezoelectric properties

A P Mirgorodsky†, M I Baraton‡ and P Quintard‡

† Institute for Silicate Chemistry, Academy of Sciences, Makarov Quay 2, 199034 Leningrad, USSR

‡ Centre d'Etude et de Recherches Céramiques, 123 avenue A. Thomas, F-87060 Limoges, France

Received 19 January 1989, in final form 2 May 1989

Abstract. An approach to lattice dynamics computations treating jointly the vibrational spectrum of a crystal and its properties relative to the uniform stress is outlined. The importance of knowing the microscopic structure of a uniform strain is emphasised. An analysis of the dynamical properties of the silicon oxynitride crystal is attempted using very restricted experimental information on its vibrational spectrum supplemented by data on its structural variations under hydrostatic pressure. Special attention is paid to changes in various structural elements, whose combined effects are treated as a vector of the uniform strain characterising its 'shape' in the space of the internal coordinates of the lattice. A set of force constants obtained by fitting the above experimental data is applied together with the estimated effective charges to predict the elastic and piezoelectric constants and also the experimentally undetermined optical frequencies.

1. Introduction: interrelations between various dynamical properties of a crystal

A model treatment of the dynamical properties of a crystal can be more or less provisionally subdivided into three sequential steps. The first step relates to the selection of the potential energy function approximation and the estimation of its parameters. The second consists of fitting experimentally determined dynamical properties and of refinement of those parameters. The third implies the use of the refined dynamical model of a crystal to predict its physical properties, which are not easily accessible by direct investigation, or to discuss their interrelations with peculiarities in the structure and bonding.

The third of the above steps is of the most practical interest from the point of view of materials science if it is treated as an aid to estimate some unknown properties of a crystal, using the available experimental information on the other properties and on the crystal structure. The efficiency of this approach strongly depends upon the uniqueness of the determination of the dynamical model parameters. Their evaluation is usually based on measurements of such macroscopic properties of a crystal as its vibrational spectrum and its elastic constants. Methods of calculating these properties have been described in a number of books (see, e.g., Born and Huang 1954).

Unfortunately, the parameters of the potential function cannot be determined in a unique way from the known macroscopic properties, and thus the scope of the above

0953-8984/89/5010053 + 14 $02.50

predictions is significantly restricted. This ambiguity has been analysed most thoroughly with respect to the problem of the determination of the force constants from the known vibrational frequencies of a crystal (Cochran 1971). These are related by

$$\omega_\lambda^2 = \boldsymbol{L}_\lambda^\dagger \boldsymbol{K} \boldsymbol{L}_\lambda \tag{1}$$

where $\boldsymbol{K}$ is the force constant matrix and $\boldsymbol{L}_\lambda$ are its eigenvectors (the 'shapes' of the normal coordinates) corresponding to the normal modes with frequencies ω_λ. One can affirm that the dynamical model is unique if it leads to a matrix $\boldsymbol{K}$ whose eigenvalues and eigenvectors coincide with experimentally determined squares of vibrational frequencies and shapes of vibrations respectively (Cochran 1971). In other words, the unique set of force constants of a crystal can be found if both the macroscopic scale characteristics of the vibrational process and its microscopic pattern are known.

In practice, only the ω_λ values are measured directly and the $\boldsymbol{L}_\lambda$ vectors cannot be determined from any experiment, although the role of isotopic effects in their characterisation is well known (including the possibility of measurement of isotopic effects in inelastic neutron scattering, as discussed by Elcombe (1974)). The additional possibility of indirect estimation of $\boldsymbol{L}_\lambda$ values originating from an IR intensity investigation and its computational treatment has also been discussed (Lazarev *et al* 1975).

In these circumstances, most attention should be paid to any additional experimental information which might interrelate directly the microscopic pattern of the structural variation in a lattice with any external field applied to the crystal if the former is treated as a response to the latter. Among such experiments, those employing the isotropic (hydrostatic) stress are promising since they provide a real opportunity to influence, and thereby investigate, the interatomic bonding in a lattice. Unlike the hydrostatic compression, the uniaxial stress often destroys the crystal at relatively low pressure and is therefore not so widely applicable.

The effect of pressure on the vibrational spectra of solids has been studied in a number of papers treating mainly the macroscopic values; Zallen (1974), for example, paid most attention to the Grüneisen parameters. Several theoretical investigations of the elasticity of a lattice have been published (see Lax 1965, Keating 1968, Barron *et al* 1971, Anastassakis and Cardona 1981) which developed and expanded the general foundations outlined by Born and Huang (1954). The experimental data on the microscopic pattern of internal strain in the particular case of the simplest diatomic cubic crystals, and their application to testing various dynamical models, have been reviewed by Cousins (1982).

Whilst at present the prospects of direct determination of the shapes of the normal vibrations seem unfavourable, the technique of crystal structure determination under high hydrostratic pressure has become routine over the last 10–15 years. The microscopic structural variations in dozens of complicated lattices have been determined precisely, as reviewed by Hazen (1985). This technique is equally applicable to powder samples for which no detailed information on the vibrational spectrum and elastic constants can be obtained. The present paper attempts to highlight the advantages of using data on the structural variation under hydrostatic compression to evaluate the dynamical model parameters of a crystal.

A crystal with N atoms per primitive cell can be regarded as a system of N interpenetrating geometrically equivalent Bravais sub-lattices, each being specified by the six primitive-cell parameters, three lengths and three angles. The relative displacements of the sub-lattices do not affect these parameters and therefore do not manifest themselves macroscopically.

A macroscopic strain of a crystal which keeps its ideal regularity is called homogeneous (Born and Huang 1954). In general, such deformation alters all primitive-cell parameters and their variations are treated as the six components of the macroscopic strain vector U_i (the use of Voigt's indices is implied). This strain changes the interatomic distances and destroys the balance of forces acting on each atom in the lattice. Thus, the lattice undergoes structural relaxation to minimise the strain energy. This process is described by the inner displacements q_k^{in} of rigid sub-lattices or by some linear combinations of normal coordinates Q_λ which correspond to the Brillouin zone centre (Anastassakis and Cardona 1981). The above quantities are related by

$$q_k^{\text{in}} = L_{k\lambda} Q_\lambda \tag{2}$$

where the coefficients $L_{k\lambda}$ are the elements of the eigenvector conjugate with the λth normal coordinate (here and below the Einstein convention of summing over repeated suffixes is assumed).

Let us recall now that the method to describe the potential function of a crystal as a sum of pair forces, three-body forces, four-body forces, etc is regarded as being one of the most suitable for lattice dynamics calculations (see, e.g., Lax 1965). Customarily the basis of such expansion consists of changing the interatomic distances, valence angles, dihedral angles, etc. These are called the internal coordinates (Califano 1976) since they are invariant to translations and rotations. The internal coordinates are used here because they provide the most easily visualised treatment of the atomic rearrangement in a lattice under compression.

At any given vector U there exists a unique way of corresponding lattice relaxation and only this vector needs to be specified to determine the structure of a strained crystal. Nonetheless, it is convenient to describe the microscopic structural variations as occurring in the space of two sets of independent variables, external strains U_i ($i = 1, 2, \ldots, 6$) and normal coordinates Q_λ ($\lambda = 1, 2, \ldots, 3N - 3$). Actually, any variation Δq_k of the kth internal coordinate may be decomposed into two contributions:

$$\Delta q_k = (\partial q_k/\partial U_i)_Q \Delta U_i + (\partial q_k/\partial Q_\lambda)_U \Delta Q_\lambda \tag{3}$$

where the subscripts Q and U denote that all Q_λ or U_i are kept constant during differentiation (Barron *et al* 1971, appendix 2). To avoid misunderstanding, it should be emphasised that in the literature on the elasticity of crystals only the second term in the decomposition (3) is referred to as the 'internal strain' or the 'internal coordinate'.

The behaviour of a crystal structure under hydrostatic compression is usually investigated by a series of x-ray or neutron diffraction experiments providing complete information on the pressure dependence of the primitive-cell parameters and atomic positions. These data can be expressed in terms of the volume compressibility κ and the linear compressibilities κ_i ($i = 1, 2, 3$), or of the compressibilities of all internal coordinates, $\mathrm{d}q_k/\mathrm{d}p$, which may be either positive or negative. The following computational scheme has been adopted to deduce the above values theoretically (Smirnov 1988, Smirnov and Mirgorodsky 1989).

The scheme is based on an expression connecting the deformation energy (per primitive cell) V with the internal coordinates q:

$$V = \tfrac{1}{2} q_k K_{kl} q_l \tag{4}$$

where K_{kl} are the force constants. The following formulae for the elastic constants C_{ij} and the volume compressibility κ may be deduced from this expression:

$$C_{ij} \equiv (1/\Omega)\,\mathrm{d}^2 V/\mathrm{d}U_i\,\mathrm{d}U_j = (1/\Omega)(\mathrm{d}q_k/\mathrm{d}U_i)K_{kl}\,\mathrm{d}q_l/\mathrm{d}U_j \tag{5}$$

where Ω is the volume of primitive cell and

$$\kappa \equiv \mathrm{d}^2 V/\mathrm{d}p^2 = (\mathrm{d}q_k/\mathrm{d}p)K_{kl}\,\mathrm{d}q_l/\mathrm{d}p. \tag{6}$$

The formal similarity of equations (5) and (6) with (1) is evident and the $\mathrm{d}q_k/\mathrm{d}U_i$ or

dq_k/dp values can be treated as the 'shapes' of the uniform strain U_i or of the hydrostatic compression respectively. However, in expressions (1) and (5) only the macroscopic values on the left-hand sides can be determined experimentally. In expression (6) the dq_k/dp values are found from the experimental microscopic pattern of hydrostatic compression and only the K_{kl} values remain unknown. Thus, the extreme importance of including this equation into the fitting procedure is evident.

Since the first three components of the vector $\boldsymbol{U}$ represent the relative changes of the linear dimensions of a crystal along Cartesian axes, the following relation is valid:

$$\kappa_i = dU_i/dp. \tag{7}$$

We can then write for dq_i/dp:

$$dq_k/dp = (dq_k/dU_i)\,dU_i/dp = (dq_k/dU_i)\kappa_i \qquad (i = 1, 2, 3). \tag{8}$$

The expression for dq_k/dU_i can be derived from (3) as

$$dq_k/dU_i = (\partial q_k/\partial U_i)_Q + L_{k\lambda}(\partial Q_\lambda/\partial U_i)_{U'} \tag{9}$$

where $L_{k\lambda} = \partial q_k/\partial Q_\lambda$ is an element of the λth eigenvector of the matrix $\boldsymbol{K}$ in a basis of internal coordinates (the subscript U' denotes that all U_i are kept constant except the variable of differentiation). It should be emphasised that the first term on the right-hand side of expression (9) does not depend upon the interatomic forces since it is specified completely by the structural parameters of a lattice.

To obtain the $\partial Q_\lambda/\partial U_i$ values, one has to use the stationary condition for energy (see Born and Huang (1954), § 11) which leads in our case to the equation

$$(\partial Q_\lambda/\partial U_i)_{U'} = -F_{\lambda i}/\omega_\lambda^2 \tag{10}$$

where $F_{\lambda i}$ is the mixed derivative of energy V against Q_λ and U_i:

$$F_{\lambda i} \equiv (\partial^2 V/\partial U_i\,\partial Q_\lambda)_{Q,U'} = (\partial q_k/\partial U_i)_Q K_{kl} L_{l\lambda}. \tag{11}$$

The expressions (9)–(10) enable equation (5) to be rewritten in a form equivalent to equation (42.2) of Born and Huang (1954):

$$C_{ij} = (1/\Omega)(\partial q_k/\partial U_i)_Q K_{kl}(\partial q_l/\partial U_j)_Q - (1/\Omega)F_{\lambda i}F_{\lambda j}/\omega_\lambda^2. \tag{12}$$

Introduction of the compliance matrix $\boldsymbol{S} = (\boldsymbol{C})^{-1}$ enables the calculation of κ_i and κ as

$$\kappa_i = \sum_j S_{ij} \qquad (i, j = 1, 2, 3) \tag{13a}$$

$$\kappa = \sum_i \kappa_i \qquad (i = 1, 2, 3). \tag{13b}$$

The inclusion of the polarisation properties of a lattice into our computational scheme is based on the expression of a polarisation vector variation $\boldsymbol{\Delta P}$ through the internal coordinates:

$$\Delta P_i = (dP_i/dq_k)\Delta q_k = z_k^i \Delta q_k. \tag{14}$$

Here i labels the Cartesian axis (as in expressions (7) and (13b)) and z_k^i is the effective charge tensor of the lattice. The formulae for the oscillator strength $4\pi\rho_\lambda^i$ of the λth normal vibration

$$4\pi\rho_\lambda^i = (dP_i/dQ_\lambda)^2 = (z_k^i L_{k\lambda})^2 \tag{15}$$

and for the piezoelectric constant e_{ij}

$$e_{ij} = dP_i/dU_j = z_k^i dq_k/dU_j \tag{16}$$

follow from expression (14).

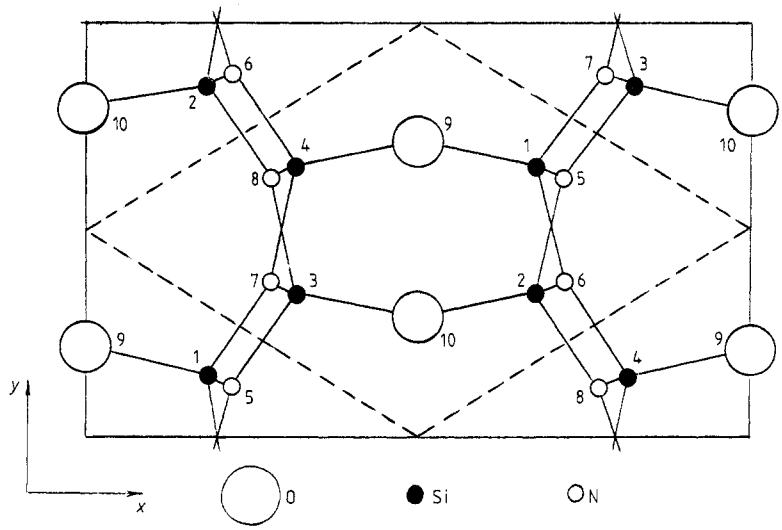

Figure 1. Crystal structure of Si_2N_2O projected onto the xy plane. A primitive cell is shown by broken lines and the atoms specifying the Bravais sub-lattices are numbered.

Thus calculation of the vibrational, elastic and polarisation properties of a crystal is possible if a set of model parameters specifying the force constant matrix $\boldsymbol{K}$ and the effective charge tensor z_k^i is determined. In the following sections an estimation of some unknown properties of a practically important material, silicon oxynitride, is attempted using a very restricted amount of spectroscopic data together with information on its structural variation under hydrostatic compression.

2. Experimental data on the structure and dynamical properties

The crystal structure of silicon oxynitride (figure 1) and its variation under hydrostatic pressure have been determined by neutron scattering from a powdered sample (Srinivasa *et al* 1977). The primitive cell of the orthorhombic ($Cmc2_1/C_{2v}^{12}$) crystal contains 10 atoms (two Si_2N_2O formula units), the silicon and nitrogen atoms occupying the general positions. Two oxygen atoms lie in the symmetry planes σ_{yz}. Each silicon atom is in a distorted tetrahedral coordination, being linked to three nitrogen atoms at distances ranging from 1.70 to 1.73 Å and to one oxygen atom at a distance of 1.645 Å. The silicon oxynitride structure can be classified as one of the framework-type lattices. One can, however, distinguish in this three-dimensional network folded sheets of $[Si_2N_2]_{\infty,\infty}$ along the yz plane, which are interconnected by Si–O–Si bridges (the two-fold coordination of oxygen) with the Si . . . Si directions along the x axis.

The available experimental data on the changes that occur in the structure under hydrostatic pressure enable evaluation of the compressibilities κ, κ_1, κ_2 and κ_3. Moreover, the changes in various fragments of the lattice can be determined and the $\partial q/\partial p$ values deduced. Some of these, corresponding to the internal coordinates involved in further treatment, are listed in table 1.

It follows in particular from the analysis of the above values that as the crystal compresses the SiOSi angles diminish and at the same time the bonds in the Si–O–Si bridges elongate. Let us recall now that similar changes in the Si–O bond lengths and SiOSi valence angles are found in other molecular systems possessing the Si–O–Si

Table 1. The internal coordinates, their equilibrium magnitudes, force constants and compressibilities.

Internal coordinates			Force constants K ($\times 10^{-6}$ cm^{-2})			Compressibilities, $\partial q/\partial p$ ($\times 10^{4}$ Å rad kbar^{-1})			
						Theoretical			
q (atoms involved)	q_e (Å deg)	Notation	I	II	III	I	II	III	Experimental (Srinivasa *et al* 1977)
Si–O	1.645	K_1	7.0	7.0	7.0	−2	−1	+2	+4
Si_1–N_5	1.70	K_2	4.2	4.2	4.2	−2	−3	−3	+10
Si_1–N_6	1.73	K_3	4.2	4.2	4.2	−2	−3	−3	−28
Si_1–N_7	1.71	K_4	4.2	4.2	4.2	−4	−4	−4	+3
N–O (various)	2.70–2.77	K_5	1.0	1.0	1.0	−4 av.	−5 av.	−3 av.	−6 av.
N–N (various)	2.78–2.84	K_6	1.0	1.0	1.0	−4 av.	−6 av.	−4 av.	−9 av.
Si–Si (various)	3.02–3.20	K_7	0	0	0	−4000 av.	−8 av.	−12 av.	−10 av.
O_9–O_{10}	3.36	K_8	0	0.15	0.15	+17200	+12	+38	+15
Si_1–O_{10}	3.30	K_9	0	0	0	+2000	−5	−2	−8
OSiN (various)	108.7 av.	K_{10}	1.0	1.0	1.0	2[a]	2[a]	2[a]	10[a]
NSiN (various)	110.6 av.	K_{11}	1.0	1.0	1.0	2[a]	2[a]	2[a]	11[a]
SiNSi (various)	119.0 av.	K_{12}	0	0	0	2000[a]	3[a]	6[a]	11[a]
SiOSi	149.5	K_{13}	0.001	0.2	0.05	−16000	−20	−44	−30
—	—	$K_{1,8}$	0	0	−0.2	—	—	—	—
—	—	$K_{1,13}$	0	0.2	0.3	—	—	—	—
—	—	$K_{8,13}$	0	−0.15	−0.05	—	—	—	—

[a] Averaged absolute variation.

bridges, as has been established by quantum chemical computations. This interrelation is represented in the force fields of these molecules by the positive sign of the off-diagonal SiO/SiOSi force constant and can be treated as originating from some intrinsic properties of the bridge. The numerical value of the force constant obtained by quantum chemical computations for molecular systems (Newton and O'Keefe 1980, O'Keefe and McMillan 1986, Ignatyev 1988) nearly coincides with the value estimated empirically for α-quartz from frequency fitting (Lazarev *et al* 1975).

Applying the above interaction force constant to the calculation of the structural variation in α-quartz under hydrostatic compression leads, however, to disagreement with experimental data. As has been shown by Jorgensen (1978), in compressed α-quartz the diminishing SiOSi angle is accompanied by a decrease in the Si–O bond lengths. No explanation of this discrepancy has been suggested as yet.

Unlike the dense α-quartz network of oxygen bridges positioned in various orientations relative to one another, with numerous non-bonding oxygen–oxygen interactions affecting the properties of the bridges, all the Si–O–Si bridges in silicon oxynitride are uniformly oriented. They lie in the symmetry planes and the two-fold axis transforms one set into another. It would be expected that in this crystal the intrinsic properties of the bridges are more readily separated from other factors affecting their dynamical properties. This is discussed below.

Experimental information on the vibrational spectrum of silicon oxynitride is restricted to the results of IR absorption measurements of a powdered specimen in the range 1300–200 cm^{-1}, (Baraton *et al* 1982). A factor-group symmetry analysis predicts the following decomposition of the representation of long-wave optical vibrations (the orientations of the transition dipoles in the polar species are indicated in brackets):

$$\Gamma^{\text{optical}} = 7A_1(z) + 6B_1(x) + 7A_2 + 7B_2(y).$$

For a qualitative understanding of the high-frequency part of the spectrum, it is reasonable to describe it in terms of the bond-stretching modes in the structural units Si–O–Si and Si–N–Si_2 composing the lattice, since the high masses of the peripheral atoms in these units favour the localisation of various modes inside the units irrespective of the peculiarities of the force field. The four Si–O stretching vibrations in two Si–O–Si bridges which are non-equivalent to translation can be approximately described as two ν_{as}SiOSi (A_2, B_1) and two ν_sSiOSi (A_1, B_2) modes similar to the corresponding ones in a free three-atomic unit. Because of the nearly plane geometry of the NSi_3 unit, its internal stretching-type modes can be described as the shifts of nitrogen in the triangle of fixed silicon atoms, each nitrogen possessing two degrees of freedom of this kind. There are in total eight long-wave optical vibrations of similar shape in the crystal, two modes in each irreducible representation. Thus, 12 optical modes are expected to be found in the relatively high-frequency region of the spectrum, nine of them being IR active.

3. The force-field model and the electro-optic scheme

In lattice dynamics computations for silicon oxynitride the potential function has been described in a basis of internal coordinates composed of the Si–O and N–Si stretching and OSiN, NSiN, SiOSi and SiNSi bending coordinates. This initial set has been complemented by the set of two-body coordinates corresponding to the non-bonding interactions at distances up to 3.5 Å. In total the basis consists of 13 sets of internal coordinates, nine two-body and four three-body ones. A complete list of equilibrium

values of these coordinates and the corresponding force constants is given in table 1. Corresponding to the number of internal coordinates, the force field has been characterised by 13 diagonal force constants (nine of bond stretching and four of angle bending type) and three off-diagonal force constants (one of stretch–stretch and two of stretch-bend type). In table 1 these are denoted by subscripts which label the force constant according to the number of coordinate set, the off-diagonal constants being labelled by two numbers of interacting coordinates.

Only diagonal force constants were included into the initial approximation of the force field. The non-zero values were originally assigned to the minimal set of them, which comprises the most easily estimated force constants of Si–N and Si–O bonds and the nearest N–N or N–O distances at the edges of the tetrahedra and of the NSiN or NSiO tetrahedral angles. None of the calculated vibrational frequencies vanished in this approximation although it was restricted practically to the internal force field of the N_3SiO tetrahedron.

The electric polarisation of a lattice induced by its deformation has been described by the simplest version of the variable-charge model (VCM) (Lazarev *et al* 1986) operating with atomic point charges which were believed to depend linearly only on the elongations of the bonds issuing from the mth atom. The parameters of this model were the charges z_m of atoms in their equilibrium positions and the derivatives of the atomic charges with respect to the bond elongations, $\partial z_m/\partial l_{mn}$ (l_{mn} is the length of the bond between the mth and nth atoms). The electroneutrality condition imposed some restrictions on the magnitudes of these parameters. For silicon oxynitride they are: $2z_{Si} + 2z_N + z_O = 0$, $\partial z_O/\partial l_{SiO} = -\partial z_{Si}/\partial l_{SiO}$, $\partial z_N/\partial l_{SiN} = -\partial z_{Si}/\partial l_{SiN}$.

All the above charge parameters were fixed in our computations since no quantitative data on the IR intensities were available. The equilibrium oxygen charge in the VCM description of α-quartz (Lazarev *et al* 1986) was of the order of one electronic charge, and it was supposed that the same value $z_O = -1e$ could be adopted for silicon oxynitride. The other equilibrium atomic charges were estimated more tentatively as $z_{Si} = 2e$ and $z_N = -1.5e$. The derivatives $\partial z_{Si}/\partial l_{SiO}$ and $\partial z_{Si}/\partial l_{SiN}$ were both assumed to be $0.6\ e/\text{Å}$. This set of charge parameters enabled the experimental IR intensity distribution to be reproduced qualitatively.

The initial set of force constants reproduced quite satisfactorily the experimental frequencies in our normal coordinate calculation. However, the elastic properties of the silicon oxynitride lattice could not be described by this force-field model since the matrix of the elastic constants was singular. This means that at this set of force constants the crystal is unstable relative to the uniform stress. Correspondingly, this set does not allow the theoretical $\partial q/\partial p$ or κ_1, κ_2, κ_3 and κ values to be calculated and compared with experiment.

It was found that at any non-zero, even extremely small magnitude of the SiOSi bending force constant (K_{13}) which slightly affected vibrational frequencies, this difficulty disappeared and the crystal became stable. The set of force constants obtained in this stage of the calculations is denoted in table 1 as set I.

A detailed comparison of the various dynamical properties of silicon oxynitride with those calculated by the above set of parameters is given in tables 1–3. The inefficiency of this version of the force field manifests itself in the huge discrepancies between the theoretical and experimental values of the compressibilities and, most obviously, in the negative signs of the off-diagonal elastic constants C_{12}, C_{13} and C_{23} which imply negative Poisson's ratios. Among the calculated $\partial q/\partial p$ values, the largest deviations from experiment were observed for the compressibility of the SiOSi angle and the $O_9 \ldots O_{10}$

Table 2. Vibrational spectra.

Experimental		Calculated			
IR spectrum ω (cm^{-1}), shape of band	Symmetry species	ω (cm^{-1}) I	II	III	$4\pi\rho\omega^2$ ($\times 10^{-4}$ cm^{-2})
1130 s	B_1	1134	1134	1134	62
	A_2	1131	1132	1131	—
1070 sh	—	—	—	—	—
1030 sh	B_2	999	999	999	1
	A_2	998	999	999	—
990 s	B_1	992	992	992	22
	A_1	927	929	929	11
953 vs	B_2	928	929	929	139
	A_2	914	914	913	—
	B_1	911	912	912	36
906 vs	A_1	894	894	894	146
730 sh	—	—	—	—	—
679 m	A_1	666	677	675	6
648 w	B_2	657	655	653	16
542 s	B_1	574	574	570	35
	B_2	554	559	560	7
	A_2	540	540	538	—
	A_1	539	565	512	6
	B_1	510	510	512	1
496 s	B_2	500	507	504	8
	A_2	468	466	462	—
448 s	A_1	425	429	427	5
	A_2	393	393	397	—
	B_1	388	388	386	1
327 m	B_2	372	393	380	1
	A_1	280	274	271	1
	A_2	270	269	267	—
252 m	B_2	210	224	229	0
	A_1	139	221	250	0

distance. This disagreement was used as a guide to the further variation of the K_{13} force constant and to the introduction of a non-zero value of the K_8 force constant characterising the stiffness of the $O_9 \ldots O_{10}$ non-bonding contact.

Furthermore, the interaction force constant $K_{1,13}$, which represented the coupled nature of Si–O stretching and SiOSi bending, was introduced based on the considerations of the force fields of the Si–O–Si bridges developed earlier (Lazarev *et al* 1975). Then, one more off-diagonal force constant, $K_{8,13}$, which represented the dynamical interaction between the SiOSi angle bending and the elongation of the $O_9 \ldots O_{10}$ distance, was found to be necessary to improve the calculated $\partial q/\partial p$ values.

The resulting force field (version II in table 1) did not significantly change the calculated frequencies with the exception of the lowest one in the A_1 species. The latter has not been identified experimentally and thus cannot be used in the refinement of the force-field model. The fitting of the experimental volume and linear compressibilities of the lattice and of the local compressibilities of its structural units has been improved considerably, as can be seen in table 1.

One more version of the force field was found when attempting to design a dynamical model which would correspond to the experimentally determined positive sign of $\partial l_{SiO}/$

Table 3. Compressibility coefficients (10^{-13} Pa^{-1}) and elastic constants (10^{10} Pa).

	κ	κ_1	κ_2	κ_3	C_{11}	C_{22}	C_{33}	C_{12}	C_{13}	C_{23}	C_{44}	C_{55}	C_{66}
Experimental	79	21	34	25	—	—	—	—	—	—	—	—	—
Calculated I	25×10^3	5×10^3	14×10^3	6×10^3	19.9	5.0	21.0	−7.4	−3.4	−5.2	9.8	8.1	8.9
II	80	19	35	26	34.3	22.0	28.6	6.4	6.1	4.2	10.8	8.9	9.8
III	110	20	54	36	31.9	16.5	25.0	4.6	3.3	0.5	9.9	8.1	9.0

Table 4. The piezoelectric constants e_{ij} (C m^{-2}) and moduli d_{ij} (10^{-12} C N^{-1}) calculated with version II of the force-field.

ij	*e*	*d*
15	−0.09	−1.02
24	0.28	−2.56
31	−0.06	−0.27
32	−0.09	−0.56
33	0.31	−1.22

∂p. The force fields I and II both led to negative compressibility of the Si–O bond in silicon oxynitride. In force field III the constant $K_{1,13}$ has increased substantially since its positive sign corresponds to the appearance of stretching forces in the Si–O bonds when the SiOSi angle decreases. Also, one more interaction constant, $K_{1,8}$, has been added. Its negative sign has been accepted in an attempt to represent the trend to elongation of the Si–O bonds as the $O_9 \ldots O_{10}$ distance increases.

The decreased (in comparison with force field II) magnitude of the diagonal SiOSi bending force constant and the total effects of varying the interaction constants $K_{1,13}$ and $K_{1,8}$ enabled a positive compressibility of the Si–O bond to be obtained when force field III was applied. In terms of absolute magnitude, however, the compressibility was still underestimated. As seen in table 3, the last set of force constants implies a considerable 'softening' of the overall lattice.

Tables 3 and 4 present the calculated values of the elastic constants C_{ij}, the piezoelectric constants e_{ij} and the moduli d_{ij} which can be treated in the absence of experimentally obtained values as theoretical estimates.

4. Discussion of results

A similarity in the calculated spectra for all of the above versions of the force field contrasts with the tremendous changes in the macroscopic elastic properties. This means that the spectroscopic data alone which are usually treated as the main source of information to effect force-field adjustments, are insufficient for the correct determination of some terms in the potential function. A description of the macroscopic elasticity of a crystal requires the precise reproduction of the potential topography for the atoms which undergo the most significant displacements in the process of uniform strain. These displacements evidently occur along the bottoms of the potential valleys and are very sensitive to the weakest interactions, both of local and non-local origin.

In particular, one can expect that the most significant changes of atomic positions in a crystal under hydrostatic pressure will be for the sites characterised by the smallest coordination numbers or by the non-uniform distribution of the surrounding atoms around a given site. The oxygen positions in silicon oxynitride satisfy these conditions. The same can be said of the bridging oxygen atoms in silica and various silicate frameworks. The macroscopic elastic properties of these crystals are determined predominantly by the parameters describing the peculiarities of a potential in which the bridging oxygen atoms move.

Since that potential is very roughly characterised by the force constants of the Si–O–Si bridge, its more precise description requires the inclusion of additional terms which would represent the much more complicated (higher-order) coordination of bridging

oxygen than is provided by the formal two-fold coordination. In the case of silicon oxynitride this implies the investigation of interactions in a relatively large area surrounding the oxygen atom which includes, in addition to the two chemically bonded silicon atoms, six nitrogen atoms in two bound N_3SiO tetrahedra and two oxygen atoms of neighbouring bridges at distances of about 3.3 Å. The possible many-bodied nature of interactions in this area may complicate the description of the potential function.

Some similarity exists between the surroundings of the bridging oxygen atom in silicon oxynitride and that in α-quartz. In the latter, at a similar value of equilibrium SiOSi angle (144°), there are six nearest-oxygen atoms in two joined tetrahedra and two other oxygen atoms removed to 3.3 Å. One can apply suitable parameters of the potential function of silicon oxynitride to α-quartz in an attempt to explain the origin of the difference in the Si–O bond length behaviour in these two crystals under hydrostatic compression.

Experimental investigation of the structure of silicon oxynitride under hydrostatic pressure (Srinivasa *et al* 1977) shows that the SiOSi angle decreases while the oxygen–oxygen distances between the neighbouring bridges increase. Under these circumstances the signs of two interaction force constants selected in version III of the force field, $K_{1,8} < 0$ and $K_{1,13} > 0$, determine their similar action on the Si–O bond length: both correspond to the forces stretching that bond at the diminished SiOSi angle and enable the experimental effect to be reproduced in the calculations. It is well known, however, that changes in the local geometry in the vicinity of the bridging oxygen atom in α-quartz under hydrostatic pressure occur in a different way: both the SiOSi angle and the length of the non-bonding oxygen–oxygen distance diminish (Jorgensen 1978). Thus, if the above interaction force constants of oxynitride were transferred into the calculation of local compression effects in α-quartz they would affect the Si–O bond length in opposite directions. Correspondingly, the experimentally determined insignificant shortening of the Si–O bond in α-quartz under compression may be treated as originating from the predominant effect of the dynamic interaction between the bond length and the non-bonding O . . . O distance.

Among the peculiarities in the macroscopic elastic properties of silicon oxynitride, the anisotropy of its compressibility deserves special comment. Qualitative speculations treating the lattice as being composed of relatively rigid sheets of $[Si_2N_2]_{\infty,\infty}$, which are interconnected by the more flexible oxygen bridges along the x axis, lead to the following relation expected for the compressibilities along the crystal axes: $\kappa_1 > \kappa_2 \simeq \kappa_3$. However, the experimental values match up as $\kappa_2 > \kappa_3 > \kappa_1$ and this result is reproduced in lattice dynamics computations irrespective of the selected version of the force field (cf table 3). A detailed analysis of the computational results shows that the stiffness of the lattice along x is determined by the large force constants of the Si–O bonds, since their directions deviate only by 15° from that axis. The calculated compressibility along the x axis can be increased considerably by assuming the Si–O force constant to decrease to values characteristic of Si–N bonds. Experimental data on the compressibility of germanium oxynitride, Ge_2N_2O, support this conclusion (Cartz and Jorgensen 1981). The linear compressibilities of this crystal match up as $\kappa_2 > \kappa_1 > \kappa_3$ and the difference from silicon oxynitride can be readily explained by smaller Ge–O force constants supposing the Si–N and Ge–N ones to be nearly the same.

The origin of the lowest stiffness of the silicon oxynitride lattice along y axis is much less evident. The lowest optical frequency of the A_1 representation corresponds to the mode with a significant contribution from SiOSi bending. This mode produces considerable negative contributions, as is determined by equation (12), to the elastic

constants C_{11}, C_{22} and C_{33}. For this mode the force $F_{\lambda 2}$ is always greater than $F_{\lambda 1}$ and $F_{\lambda 3}$. Correspondingly, the mechanical compliance of the lattice along y (the linear compressibility κ_2) is the greatest. Thus, while the largest stiffness along x is explained very pictorially by the examination of the static stresses arising in the uniformly strained lattice, the lowest stiffness along y is connected with the peculiarities of the shape of the normal coordinate with the lowest energy.

The experimental compressibilities of the SiN_3 groupings are rather badly reproduced in our calculation because of the oversimplified description of the corresponding part of the potential function. The deficiency of the force-field model in describing these groupings manifests itself more clearly in the calculation of the $\partial q/\partial p$ values than of the vibrational frequencies. This is probably due to some averaging of individual errors when estimating several force constants to determine each of the vibrational frequencies. A more sophisticated force-field model of these groupings can be designed using the extended set of experimental data including the $\partial q/\partial p$ values for similar crystals like Si_3N_4 (Cartz and Jorgensen 1981).

Of the calculated magnitudes of the macroscopic elastic and piezoelectric constants (or moduli), those obtained with the set II force constants seem to be the most reliable since this set enables better reproduction of the experimental compressibility. Although the probable errors of such predictions can hardly be estimated, their success in similar calculations for silicon dioxide and some other crystals leads one to expect that the signs and at least the orders of the values of the above quantities are predicted correctly.

5. Concluding remarks

Although only a single example of a joint treatment of the vibrational spectrum and the local compressibilities of various structural fragments has been investigated in this paper, some general conclusions can be deduced. To a certain extent, these two sources of information on the potential function are complementary in nature. The compliance of a crystal to mechanical stress, characterised macroscopically by its compressibility and microscopically by the $\partial q/\partial p$ values, determines predominantly the terms of the potential function which correspond to relatively weak interactions at large distances. Conversely, the vibrational frequencies, much less sensitive to the above interactions, are determined mainly by the forces arising in the chemical bonds and the valence angles.

Numerous complex oxides with network-type structures are thought at present to be promising for practical use due to their elastic, opto-acoustic or electro-acoustic properties. The present investigation has shown the importance of oxygen bridges in the origin of these properties and the inefficiency of the oversimplified models of purely valence forces to describe the potential which governs the movements of the oxygen atom. This potential is shown to be equally dependent on the electronic structure of the oxygen bridge itself and on the interactions of oxygen with several relatively distant atoms. The interactions between distant atoms constitute the most variable part of the potential function which specifies the peculiarities of the given lattice. Thus, the quantum chemical calculations for molecular systems containing oxygen bridges, which are presently rather widely applied to the investigation of bonding in appropriate crystals, need care in their application to the properties relevant to the uniform strain of a lattice.

References

Anastassakis E, Cardona M 1981 *Phys. Status Solidi* b **104** 589
Baraton M I, Labbe J C, Quintard P 1982 *J. Mol. Struct.* **79** 333

Barron T H K, Gibbons R G and Munn R W 1971 *J. Phys. C: Solid State Phys.* **4** 2805
Born M and Huang K 1954 *Dynamical Theory of Crystal Lattices* (London: OUP)
Califano S 1976 *Vibrational States* (New York: Wiley)
Cartz L and Jorgensen J D 1981 *J. Appl. Phys.* **52** 236
Cochran W 1971 *Acta Crystallogr.* A **27** 556
Cousins C S G 1982 *Solid State Commun.* **44** 1205
Elcombe M M 1974 *J. Phys. C: Solid State Phys.* **7** L202
Hazen R M 1985 *Microscopic to Macroscopic (Reviews in Mineralogy* vol 14) ed. S W Kieffer and A Navrotsky (Washington: Mineralogical Society of America) p 317
Ignatyev I S 1988 *J. Mol. Struct.* **172** 139
Jorgensen J D 1978 *J. Appl. Phys.* **49** 1476
Keating P N 1968 *Phys. Rev.* **169** 758
Lazarev A N, Mirgorodsky A P and Ignatyev I S 1975 *Vibrational Spectra of Complex Oxides* (Leningrad: Nauka)
Lazarev A N, Mirgorodsky A P and Smirnov M B 1986 *Solid State Commun.* **58** 371
Lax M 1965 *Lattice Dynamics* ed. R F Wallis (Oxford: Pergamon) p 583
Newton M D, O'Keefe M and Gibbs G V 1980 *Phys. Chem. Minerals* **6** 305
O'Keefe M and McMillan P F 1986 *J. Phys. Chem.* **90** 541
Smirnov M B 1988 *Optika i Spectroskopya* **65** 311 (in Russian)
Smirnov M B and Mirgorodsky A P 1989 *Solid State Commun.* at press
Srinivasa S R, Cartz L, Jorgensen J D, Worlton T G, Beyerlein R A and Billy S 1977 *J. Appl. Crystallogr.* **10** 167
Zallen R 1974 *Phys. Rev.* B **9** 4485